Removal of Textile Dyes on a Biosorbent Based on the Leaves of *Atriplex Halimus*

Douara, Nadia; Benzekri Benallou, Moukhtar*[+], Termoul, Mourad; Mekibes, Zohra; Bestani, Benaouda; Benderdouche, Nouredine

Laboratory of SEAMM, University of Mostaganem, P.B. 227, Mostaganem, ALGERIA

ABSTRACT: *The objective of this study is to characterize the Biosorbent (Atriplex Halimus leaves) and its application in the removal by adsorption of anionic and cationic dyes known for their toxicity such as Bemacid Blue (BB), Bemacid Red (BR), and Methylene Blue (MB) contained in water. The Atriplex Halimus was characterized by Boehm's method, FT-IR, XPS, SEM, pH Zero Charge Point (pH_{ZPC}), iodine value, and Methylene Blue value. The tests carried out in this experiment showed that the Biosorbent can remove Bemacid Blue (BB), Bemacid Red (BR), and Methylene Blue (MB). The effect of several parameters such as pH of the solution, biomass dose, contact time, initial concentration of dye used, and the temperature was studied in a batch system. The adsorbate-adsorbent equilibrium times are reached after 60 min for MB and 90 min for BB and BR. The adsorption is maximal for an adsorbent dose of 8 g/L for the three dyes. The best retentions were observed at pH 11, 6.45, and 5.12 for MB, BB, and BR respectively. The maximum adsorption capacities are 289.8, 29.7, and 32.9 gm/L for Methylene Blue (MB), Bemacid Blue (BB), and Bemacid Red (BR) respectively. Modeling of the experimental data showed that the Langmuir and pseudo-second-order models describe, respectively, the adsorption isotherms and the kinetics in a satisfactory way. The study of the thermodynamic aspects showed that the adsorption of the three dyes by the leaf biomass of Atriplex Halimus is a favorable, exothermic, and spontaneous phenomenon.*

KEYWORDS: *Biosorbent; Atriplex halimus; Bemacid blue; Bemacid red; Methylene blue.*

INTRODUCTION

More than 10,000 different dyes have been commercialized to date and their annual production exceeds $7x10^5$ metric tons [1]. Dyes are used in the coloring process of various industrial materials such as dyes, textiles, plastics, cosmetics, paper, and leather [2] pose pollution problems in the form of colored wastewater discharges into environmental water bodies [3]. These discharges present a real danger for man and his environment because the dyes can exert acute and/or chronic effects on the organisms that are exposed to them according to the concentration and the duration of exposure. Dyes are very visible, and at very low concentrations, they can give an abnormal coloration to surface waters, which attracts the attention of the general public. Dye-polluted waters reflect sunlight, which affects the growth of living things and disturbs their biological activities. Dyes in wastewater undergo chemical and biological changes, which lead to an overconsumption of dissolved oxygen and destroy aquatic life.

***** *To whom correspondence should be addressed.*
+ *E-mail: benzekrimokhtar@yahoo.fr*
1021-9986/2022/10/3646-3661 16/$/6.06

Synthetic dyes have a high potential for resistance to discoloration when exposed to light.

The elimination of these pollutants from industrial discharges is very often carried out by conventional chemical treatments such as decantation, coagulation-flocculation, oxidation... The wastewater that is treated by these processes still contains pollutants and is loaded due to the number of added reagents. In most cases, these processes are very expensive. It is necessary to think about more efficient and less expensive solutions.

Adsorption techniques have been successful in the removal of organic species. Currently, activated carbon is the most used adsorbent due to its adsorption potential which is very important for dyes, but it has the disadvantage of being expensive due to its preparation which requires large investments (grinding, sieving, activation, ...).

The main advantages of these biomaterials are their reusability, efficiency, and low operational cost. In recent years, many studies have shown that the biosorption of dyes by different materials has already been reported, on biomasses such as De-oiled Algae [4], Peanut shells [5], Brewery waste [6], Luffa cylindrica [7], Mussel shells [8], Pinus radiate [9], Calcined lotus leaf [10], Eucalyptus [11] globulus, Cynara cardunculus, and Prunus cerasefera [12]. It is in the work that we have been interested to test a new adsorbent (leaves of the Atriplex Halimus) non-conventional low cost for the treatment of water contaminated by textile dyes.

To this fact, we studied the physical parameters such as the initial concentration of the three pollutants, the pH, the temperature, the dose of adsorbent, and the capacity of a biomass (leaves of Atriplex Halimus) for the biosorption of the three textile dyes (Blue bemacid, Red bemacid and Blue of methylene) A modeling of the biosorption equilibrium isotherm, the kinetics, and the thermodynamic parameters was performed to better understand the mechanism of dye adsorption on biomass (leaves of Atriplex Halimus).

EXPERIMENTAL SECTION

Preparation of the adsorbent

In this work, we chose to valorize the leaves of Atriplex Halimus for the removal of some organic pollutants. The biosorbent used in this study was prepared according to the experimental protocol developed in the laboratory.

The leaves of Atriplex Halimus were crushed and sieved to a diameter of 0.14 mm and then washed with a Soxhlet extractor to remove the active principle. Then were dried in the oven for 24 h at 80 °C. After drying in the oven, the materials were crushed and sieved to a diameter < 71 µm because it has the finest particle size available in the laboratory. Finally, the biosorbent was kept in an airtight container.

The studied adsorbates

We chose three textile dyes which are Methylene Blue (MB), Bemacid Blue E-TL (BB), and Bemacid Red E-TL (BR).

Methylene blue, a cationic dye (Basic Dye), is chosen as a representative model for medium-sized organic pollutants. It is a molecule that is also used to test the adsorption capacity of solids [13-14], and to determine their specific surface [15].

It is widely used in several fields such as chemistry, pharmaceuticals, cosmetics, and the textile industry.

The two acid dyes (the Blue Bémacide E-TL and the Red Bémacide E-TL) are used in the form of salt belonging to the category of the water-soluble dyes, they were given to us by the company of production of artificial silk of SOITEX Tlemcen, Algeria. These dyes are used for textile dyeing and more particularly for polyamide fibers.

Characterization Techniques

Iodine Index and Methylene Blue Index

The iodine index is a widely used parameter to characterize activated carbon due to its simplicity and rapid evaluation of activated carbon quality [16]. The existence of micropores and mesopores of biosorbent was also estimated by iodine index (ASTM D4607-94 method) [17], and methylene blue index (Chemviron Carbon company TM-11 method) [18-19], respectively.

Zero Charge Point pH (pH_{PCZ})

The pH_{PCZ} or pH of the zero or zero charge point is the pH value for which the charge on the surface of the carbon is zero. The neutral surface charge (pHpzc) was determined by the pH drift technique [20].

A volume of 50 mL of NaCl solution (0.01 M) is placed in stoppered bottles, the pHi (initial pH) is adjusted from 2 to 12 by adding sodium hydroxide or 0.1 N hydrochloric acid; then 0.15 g of adsorbent is added to the NaCl

solutions. After 48 hours of stirring the pH_f (final) is measured. The ΔpH is plotted against the pH_i (initial). The pH that corresponds to the point of intersection with the abscissa axis is the pH_{PCZ} of the biosorbent.

Boehm's method

A Boehm titration was performed to determine the number and type of oxygen groups on the surface [21-22]. The adsorbent was reduced to powder form and then contacted with one of the following three bases and one acid: $NaHCO_3$, Na_2CO_3, NaOH, and HCl. After filtration of the suspension, the excess of base is dosed by a solution of HCl (0.1N). From the titration curves, the type of site contained in the activated carbon is deduced by Boehm's classification. Masses of 0.3 g of the tested adsorbent were successively put in vials with caps. To each vial, 50 mL of each base and an acid of concentration 0.1 N were added and stirring was maintained for 72 hours at the temperature of (25 ± 2) °C. After filtration, the amount of base consumed by the Biosorbent is determined by titration of a known volume of filtrate (10 mL) with hydrochloric acid (0.1 N).

FT-IR, XPS, and Scanning Electron Microscopy (SEM) methods

The surface chemical functions are determined by FT-IR and XPS methods.

FT-IR spectra were recorded in the range (400-4000 cm^{-1}) using a SHEMADZU - pristig-21 spectrometer. X-ray Photoelectron Spectroscopy (XPS) is a powerful technique for qualitative and quantitative characterization of surfaces [23]. XPS measurements were performed on a Kratos

Axis Ultra using an Al Kα X-ray source (hv = 1486.6 eV) [24].

Scanning Electron Microscopy (SEM) was performed to show the pore structure of the studied biomass.

Batch biosorption experiments

Effect of equilibrium time

To determine the sufficient time to reach equilibrium, a kinetic study is necessary. We prepared two solutions of concentrations 30 and 50 mg/L. In a series of beakers, 0.1 g of biosorbent and 25 mL of solution of the studied adsorbate are added in each beaker. The whole is stirred at stirring times from 15 to 240 minutes, then centrifuged (Hettich EBA 8) at 6000 rpm and analyzed by spectrophotometry (Shimadzu UV mini - 1240), with the wavelengths are 665, 609, and 504 nm for methylene blue, bemacid blue and bemacid red, successively.

Influence of the quantity of biomass

Another factor influencing the adsorption properties is the dose of biosorbent which is particularly important because it determines the degree of adsorption.

A volume of 25 mL of study solution of known concentration (100 mg/L for MB and 50 mg/L for BB and BR) was mixed and stirred with 0.05, 0.1, 0.15, 0.2, 0.25, 0.3, 0.35, and 0.4 g of study biosorbent, respectively, for a time that was determined beforehand. After filtration, the solution was analyzed to determine its concentration which will allow the determination of the percentage of elimination of the substance to be fixed.

Influence of the pH of the solution

The initial pH of the solution is an important parameter that must be considered in any adsorption study [25]. We monitored the effect of pH (2 to 11) on the adsorption of each dye for an initial concentration of 100 mg/L (BM) and 50 mg/L (BB and RB) and a mass of 0.2 g of biosorbent by adjusting the initial pH with NaOH (0.1 N) and HCl (0.1 N) solutions, for the different pH values studied.

Adsorption Isotherms

The adsorption isotherm characterizes the adsorption process and expresses the quantity of adsorbate present on the adsorbent q_e (expressed in mg per g of adsorbent).

In a series of beakers containing 25 mL of concentrations between 100 mg/L and 1000 mg/L. After the stirring time, the biomass was separated by centrifuge and the adsorbents (Methylene Blue, Bemacid Blue, and Bemacid Red) in solution were determined by spectrometry. The adsorption capacity (q_e) and percent removal R(%) are determined by the following equations [26-27]:

$$q_e = \frac{(C_0 - C_e)}{m} * V \quad (2)$$

$$R(\%) = \frac{(C_0 - C_e)}{C_0} \times 100 \quad (3)$$

Where: C_0 : initial concentration of the adsorbate (mg/L) ; C_e : equilibrium concentration of the adsorbate (mg/L) ; m : mass of adsorbate (g) ; V : volume of adsorbate (L).

Determination of the maximum adsorption capacity for the three dyes studied on the leaves of Atriplex Halimus, the experimental data were correlated by *Langmuir* [28], *Freundlich* [29], and Temkin [30-31] isotherms. These isotherms can be written as the following equations:

$$q_e = \frac{q_m \times K_L \times C_e}{1 + K_L \times C_e} \quad (4)$$

$$q_e = K_F \times C_e^{1/n} \quad (5)$$

$$q_e = B_T \times \ln(K_T \times C_e) \quad (6)$$

Where: q_m: the maximum adsorption capacity (gm/L); K_L: constant of the Langmuir isotherm; K_F, n: constants of the Freundlich isotherm; K_T: Temkin isotherm constant (L/mg) (the retention capacity at equilibrium); $B_T=(R\times T)/b_T$]; R: constant of perfect gases (8.314 J/mol.K); T: absolute system temperature (K); b_T: is the heat of sorption in (J/mol).

Kinetic studies

The pseudo-first-order equation (10) [32], the pseudo-second-order Equation (11) [33], and the intraparticle diffusion model equation (12) [34] were tested by the following equations:

$$\ln(q_e - q_t) = \ln(q_e) - (k_1 \times t) \quad (10)$$

$$\frac{t}{q_t} = \frac{1}{k_2 \times q_e^2} + \frac{t}{q_e} \quad (11)$$

$$q_t = k_i \times t^{0.5} + C \quad (12)$$

Where: q_e and q_t: adsorption capacity of the adsorbate (gm/L) at equilibrium and at time t (min); k_1 and k_2: kinetic constant of the pseudo-first-order and the pseudo-second-order; k_i: intraparticle diffusion rate constant; C: constant.

Study of the influence of temperature

The influence of temperature on adsorption has been carefully studied, to study the effect of temperature on the adsorption of dyes by the biomass studied, we have chosen the following temperatures: 25, 30, 35, and 40 °C. Thermodynamic parameters show the feasibility and spontaneous nature of a biosorption process. These parameters are determined using the following equations [35-36]:

$$\Delta G° = -R \times T \times \ln(K_d) \quad (7)$$

$$\Delta G° = \Delta H° - T\Delta S° \quad (8)$$

$$\ln(K_d) = -\frac{\Delta H°}{R \times T} + \frac{\Delta S°}{R} \quad (9)$$

Where: K_d: thermodynamic distribution capping; $\Delta G°$: Gibbs energy (kj/mol) ; $\Delta H°$: standard enthalpy (kJ/mol) ; $\Delta S°$: standard entropy (kJ/mol.K).

As criteria for fitting quality, the Chi-Square parameter (χ^2), Root Mean Square Error (*RMSE*), and Average Relative Error (ARE) [37]. The functions are defined as follows:

$$ARE = \frac{100}{n}\sum_{i=1}^{n}\left[\frac{|q_{exp} - q_{cal}|}{q_{exp}}\right]_i \quad (10)$$

$$\chi^2 = \sum_{i=1}^{n}\left[\frac{(q_{exp} - q_{cal})^2}{q_{cal}}\right]_i \quad (11)$$

$$RMSE = \sqrt{\frac{1}{(n-2)}\sum_{i=1}^{n}(q_{exp} - q_{cal})^2} \quad (12)$$

RESULTS AND DISCUSSION

Characterization

Iodine number and methylene blue index

The iodine number can reflect the ability of CA to adsorb small molecules from a liquid [38].

The iodine number characterization test (Table 1), show an impotent microporosity (425.2 mg/g). This was followed by the methylene blue index test to determine the existence of micropores and mesopores in the biosorbent studied [16]. The methylene blue index cited in Table 1 indicates that the Atriplex Halimus biosorbent at a mesopore is significant (119.5 mg/g).

pH_{PCZ} and Boehm's method

The pH_{PZC} corresponds to the pH value for which the net surface charge of the adsorbent is zero. The results obtained are shown in Fig. 1 and Table 2.

The pH value at the zero charge point (pH_{PZC}) is obtained at the intersection of the initial pH with the final pH. Fig. 1 shows that the pH_{PZC} of the studied biosorbent is acidic 6.25. This is in agreement with the Boehm titration results (Table 2) for the Atriplex Halimus biosorbent showing the presence of acidic functional groups.

Table 1: Results of iodine number and MB index and pH_{ZPC} of studied biosorbent.

Iodine number (mg/g)	MB index (mg/g)	pH_{ZPC}
425.2	119.5	6.25

Table 2: Chemical groups on the surface of biosorbent (Boehm method).

Carboxylics (meq-g.g^{-1})	Laconics (meq-g.g^{-1})	Phénolics (meq-g.g^{-1})	Acids (meq-g.g^{-1})	Basics (meq-g.g^{-1})
0.952	0.068	1.769	2.789	1.247

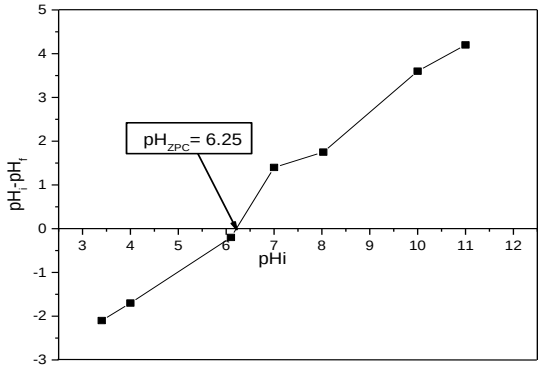

Fig. 1: Determination of pH_{PCZ} of biosorbent.

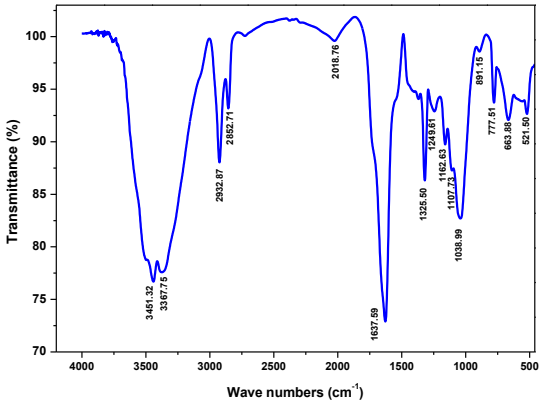

Fig. 2: FT-IR spectrum of Atriplex Halimus biosorbant.

At pH below 6.25, the biomass surface has a positive charge, while above pH 6.25 will have a negatively charged surface. This factor may be of great importance in the adsorbate-adsorbent interactions in the liquid phase. Cation adsorption is favorable at pH> pH_{PZC}, on the other hand, anion adsorption is favorable at pH < pH_{PZC} [39].

FT-IR spectral analysis

FTIR characterization allows the detection of the different functional groups that exist in the biosorbent.

The peaks in the FTIR spectrum of the Atriplex Halimus-based biosorbent are identified with various groups and bonds based on their wavenumbers in cm^{-1}, as reported in the literature [40-42].

Fig. 2 shows the FT-IR spectrum of biosorbent the O-H bond that corresponds to alcohols, phenols, and chemisorbed water is located in the Bend between 3600 and 3200 cm^{-1} [43]. The two high wavenumber bands at 3451.32 and 3367.75 cm^{-1} are the asymmetric and symmetric elongations of an NH_2 group. The two CH_2 vibrational bands at 2932.87 and 2852.71 cm^{-1} are attributed to asymmetric and symmetric elongations of C-H in CH_2, respectively [44]. A peak at 1720.5 cm^{-1} represented the C=O elongation vibration of a carboxylic acid, a thin peak appearing at 1637.59 cm^{-1} confirms the presence of an amide group [45] indicating the presence in the biosorbent.

A band at 1162.63 cm^{-1} corresponding to the C-O bond of the aliphatic ester group. Several bands between 1325.5 to 1039 cm^{-1} represent the C-O bond of phenols [46]. The peak at 1107.73 cm^{-1} corresponds to the C-O stretching vibration and the O-H bending modes of the alcoholic, phenolic and carboxylic groups [47]. The FT-IR data have confirmed the composition of the organic matter, carboxylic groups, and phenolic groups present on the biosorbent.

XPS analysis

We characterized the Atriplex Halimus biosorbent by XPS. Fig. 3 shows the XPS spectra of the Atriplex Halimus-based biosorbent (C1s, O1s, and N1s). The C1s carbon peak consists of C=O bonds (carboxyl groups) at 288.4 eV, single C-O or C-N bonds at 287.5 eV, C-O bonds at 286.1 eV, and C-C bonds at 284.5 eV [24]. The O1s peak is characterized by 4 components at 532.8, 532.3, 531.9, and 531.2 eV corresponding respectively to C-O-C

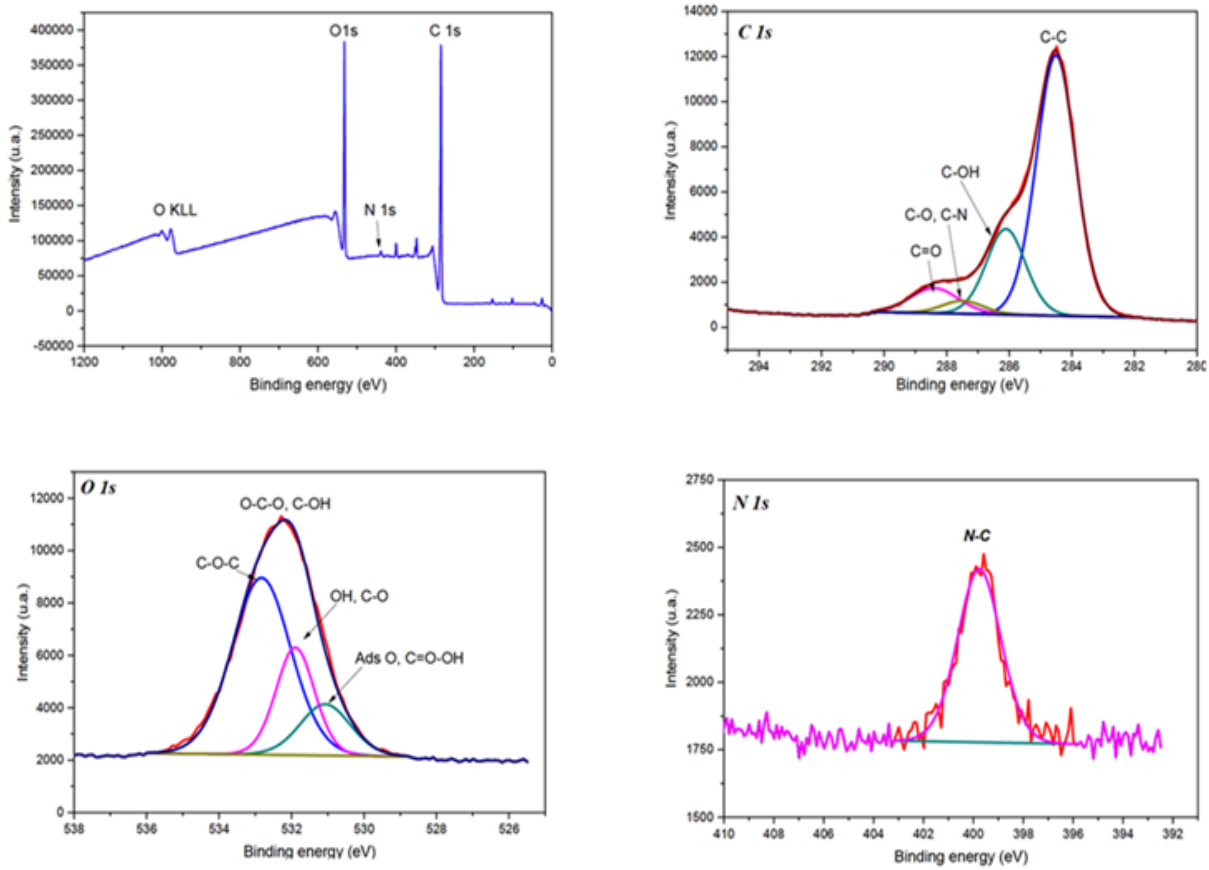

Fig. 3: XPS spectra of Atriplex Halimus biosorbent (C1s, O1s and N1s).

(ether oxide groups), C-OH (contribution of C-OH already identified in the C1s peak), O-H (hydroxide groups) or C-O (carbonyl groups) (contribution of C=O already identified in the C1s peak) and O=C-OH and oxygen chemisorption [24], respectively. Finally, the N1s peak is a single component at 399.8 eV with a single C-N bond that matches from amine or amine (contribution of C-N already identified in the C1s peak). This analysis confirms the results of FT-IR spectrum analysis.

Scanning Electron Microscopy (SEM)

The surface morphology of the biomaterial (Atriplex Halimus) was thus observed by SEM. The pictures obtained by scanning electron microscopy are presented in Fig. 4. The SEM image (Fig. 4) shows a structure some porosity of the biomaterial (Atriplex Halimus) with pores of more or less diverse shapes and sizes. This figure also indicates the presence of a variety of cavities on the external surface. These can explain the important surface of biomass.

Batch biosorption

Effect of adsorption time

The effect of stirring time was a critical factor in the sorption experiments as the data will help confirm the stirring time to reach equilibrium in the adsorption process [48].

The results obtained are represented graphically in Fig. 5. It can be seen that from Fig. 5 the removal rates of Methylene Blue (MB), Bemacid Blue (BB), and Bemacid Red (BR) by the biosorbent (Atriplex Halimus) increases with time for the two chosen concentrations until a saturation level is reached after 60 min for Methylene Blue and 90 min for Bemacid Blue and Bemacid Red.

The effect of adsorbent dose on adsorption

The effect of the biosorbent dose on the removal rate of the three pollutants (MB, BB, and BR) is shown in Fig. 6. The percentage removal of the pollutants increases with the increase of the adsorbent dose [49] (2 to 8 g/L).

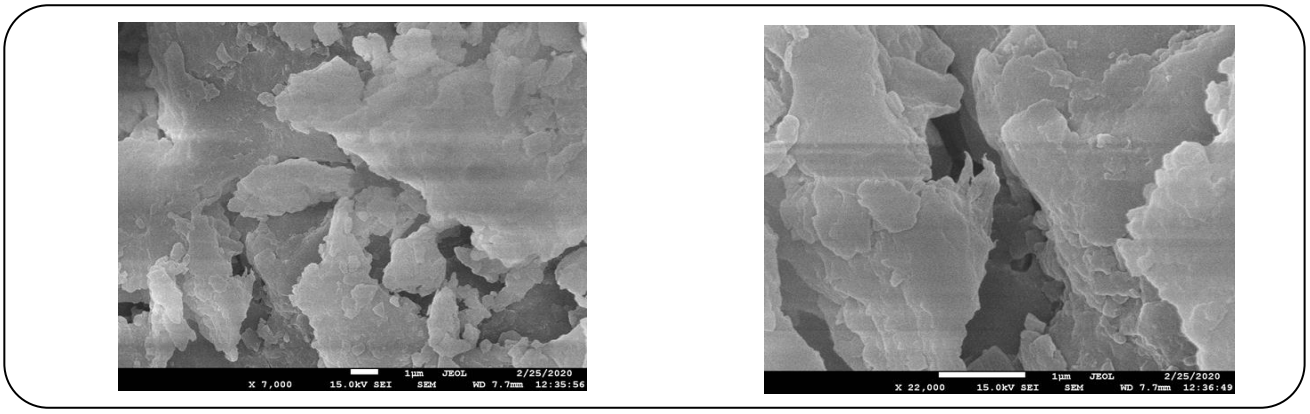

Fig. 4: SEM image of biosorbent (Atriplex Halimus).

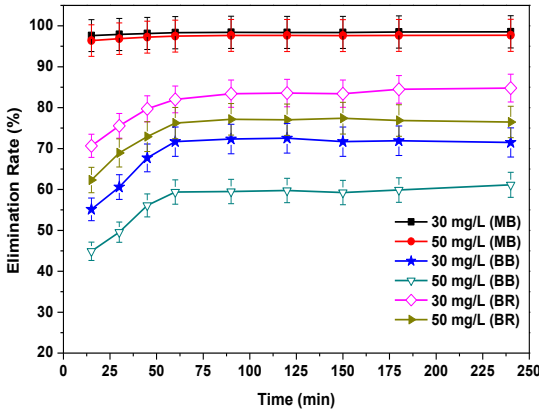

Fig. 5: Removal rates of the three dyes studied as a function of time.

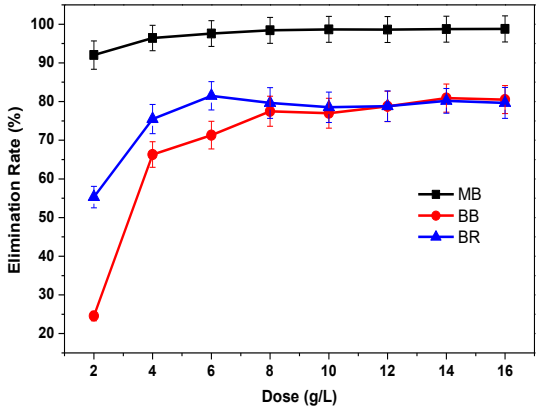

Fig. 6: Removal rate of Methylene Blue, Hemacid Blue, and Hemacid Red.

From the dose of 8 g/L, the percentage of removal remains almost constant until 16 g/L. The amount of adsorption for the three pollutants increases with the increase of the dose

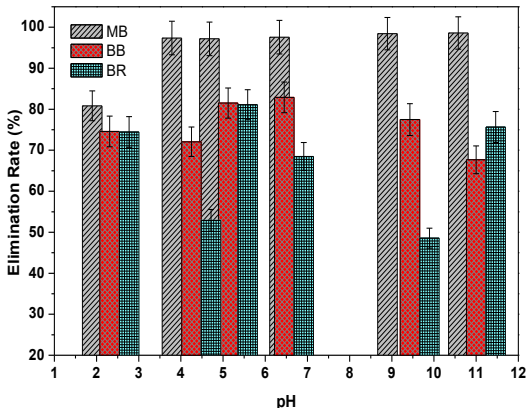

Fig. 7: Removal rates as a function of pH for the three dyes.

of biosorbent until the dose of 8 g/L and decreases between 8 to 16 g/L. Thus, the adsorption is maximal for an adsorbent dose of 8 g/L for the three dyes. Therefore we will take this optimal dose for all adsorption experiments.

Influence of pH

The adsorption results are represented graphically in Fig. 7. It can be observed on this figure that the best retention rates are obtained at pH 11, 6.45, and 5.12 for Methylene Blue, Bemacid Blue, and Bemacid Red respectively.

This phenomenon could be explained by the fact that at a high acidic pH value, a strong electrostatic attraction exists between the surface of the positively charged adsorbent and the anionic acid dye. When the pH of the system increases, the number of negatively charged sites increases, and the positively charged ones decrease. Also, the adsorption of the acid dye at alkaline pH is due to the presence of an excess of hydroxyl ions, which compete

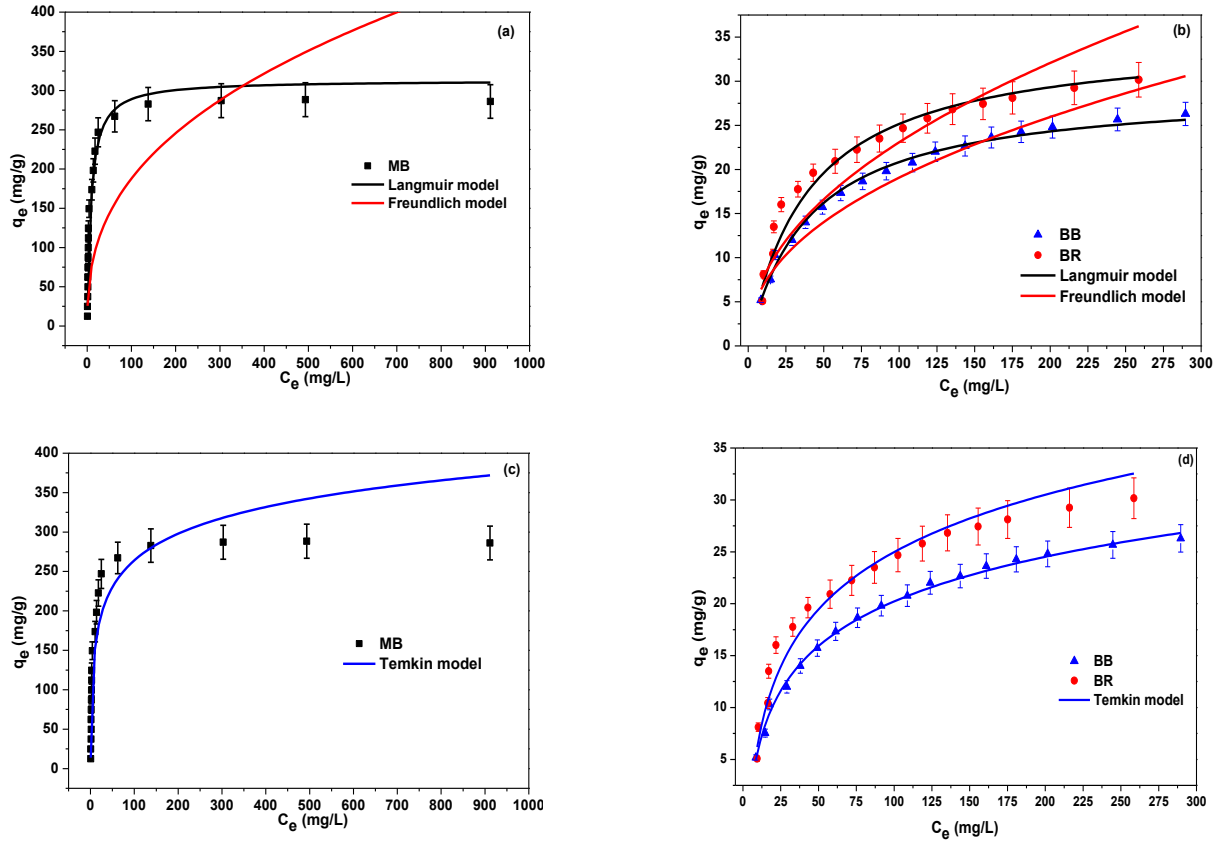

Fig. 8: Adsorption isotherm of three dyes (MB, BB,and BR), (a) Langmuir and Freundlich model for MB, (b) Langmuir and Freundlich model for BB and BR, (c) Temkin model for MB and (d) Temkin model for BB and BR.).

with the anions of the acid dye for the adsorption sites [50-51] as is the case with biomass (Atriplex Halimus). Cation adsorption is favored at pH > pH_{PCZ}; anion adsorption is favored at pH < pH_{PCZ}. Under these conditions, the adsorption of the anionic dye is supported by an acidic environment [52].

Biosorption isotherm

The results of this study are shown in Fig. 8 and summarized in Table 3. From Fig. 8, we observe that from the adsorption isotherms of MB, BB, and BR on a biosorbent, the quantity of the pollutants increases more or less quickly for low concentrations in solution, then attenuates to reach a plateau formed corresponding to a saturation of the adsorption sites, and translating an adsorption in monolayer. The obtained isotherm is of type L according to the classification of Giles [53]. Langmuir, Freundlich and Temkin isotherms were used to examine the experimental data.

The non-linear form of the Langmuir isotherm (Fig. 8) is more effective in representing and explaining the adsorption data, i.e. adsorption is limited to the monolayer coverage and the surface is homogeneous in functional groups with significant interaction with the three pollutants and the biosorbent. Table 3 gives the equations of the lines obtained as well as the constant correlation coefficients (R^2) are higher than 0.97, and the χ^2, ARE, and RMSE parameters are fairly small so there is not a great difference between the experimental and Langmuir model-calculated adsorption quantities for the three dyes. The latter is confirmed that this system is well described by the Langmuir model for the three dyes with a maximum adsorption capacity of 289.8, 29.72 and 29.72 gm/L for the trio of dyes Bleu de Methylene, Bemacid Blue and Bemacid Red, respectively.

The characteristics of the Langmuir isotherm are expressed from the equilibrium parameter R_L: ($R_L=1/(1+K_L\times C_0)$). The value of R_L indicates whether

Table 3: Langmuir, Freundlich and Temkin parameters of the adsorption of the three dyes on a biosorbent (Atriplex Halimus).

Langmuir	q_m (mg.g^1)	K_L	R^2	ARE(%)	RMSE	Chi-Square (χ^2)
BR	32.9	0.0329	0.9769	6.8325	0.6809	1.8389
BB	29.7	0.0235	0.9940	2.9596	0.2185	0.4269
MB	289.8	0.1917	0.9926	9.5568	10.1951	17.5669
Freundlich	1/n	K_F	R^2	ARE(%)	RMSE	Chi-Square (χ^2)
BR	0.3429	4.8465	0.9238	14.0822	2.2491	5.1334
BB	0.3615	3.6659	0.9605	9.3297	1.0871	2.1522
MB	0.1978	91.428	0.7704	53.2789	48.3947	300.026
Temkin	b_T	K_T	R^2	ARE(%)	RMSE	Chi-Square (χ^2)
BR	346.71	0.3259	0.9762	7.6429	0.7790	1.9744
BB	389.63	0.2567	0.9959	4.07312	0.2578	0.4034
MB	58.485	4.3490	0.9063	23.3372	30.4877	100.299

the isotherm is unfavorable (R_L>1), linear (R_L =1), favorable (0< R_L<1) or irreversible (R_L = 0) [54]. R_L values calculated from the Langmuir constant K_L, which were between (0.0016 to 0.0495) for MB, (0.0784 to 0.4598) for BB and (0.0573 to 0.3781) for BR. The Langmuir R_L separation parameter less than 1 and greater than 0, indicates that the adsorption of MB, BB, and BR on the studied biosorbent is favorable.

The values of the Freundlich constant (1/n) between 0 and 1 for MB, BB, and BR are 0.1978, 0.3615, and 0.3429 respectively, which were considered as the intensity factor indicating the adsorption is favorable [45]. Application of the Temkin model for the obtained experimental results gives a good nonlinear fit with R^2 correlation coefficients between (0.97 - 0.99) and the χ^2, ARE, and RMSE parameters are fairly small for acid dyes (BB and RB). The Temkin constants K_T which is the equilibrium binding constant and the B_T constant related to the heat of adsorption are reported in Table 3. According to the Temkin isotherm, b_T values < 20 J/mol are attributed to physisorption dominating chemisorption [55]. The adsorption process is considered chemisorption of an adsorbate on the biosorbent. Similar observations have been reported in the literature [56].

Table 4 represents a comparison of the adsorption capacity of Atriplex Halimus biosorbent obtained in this study with other adsorbents obtained in the literature for the adsorption of MB, RB and BB. It shows that the biosorbent Atriplex Halimus can be a promising material for the elimination of methylene blue, bemacid blue and methyl bemacid red, also compared to other adsorbents.

Adsorption kinetics

Three kinetic models are considered to study the adsorption process of Methylene Blue and Red Bemacid. The adsorption tests are carried out by taking contact times lower than the equilibrium time for the biomass (Atriplex Halimus) kinetic models are used to study the adsorption process of the three preceding dyes.

For this, we followed the adsorption kinetics for the three dyes with an initial concentration of 100 mg/L in contact with a mass of 0.1 g of Biosorbent for Methylene Blue, Bemacid Blue, and Bemacid Red.

From these results we will notice that the adsorption of the three dyes by our Biosorbent (Atriplex Halimus) takes the Pseudo-second order adsorption kinetics with correlation coefficients are higher than 0.996 for the three dyes (Methylene Blue, Bemacid Blue, and Bemacid Red) and experimental capacities are very close to the one determined implies that all this still justify that the adsorption kinetics of MB, BB and BR used by a biosorbent is of this order.

The results of the adsorption kinetics in some recent works for other systems show that the pseudo-second-order perfectly represents the experimental data in many cases [65]. The values of q_e calculated with the pseudo-

Table 4: Comparison of biosorption performance of Atriplex Halimus for removal of dyes (MB, BB and BR) with some other adsorbents.

dyes	Adsorbents	Max. Capacity (mg/g)	References
MB	Copper vanadate	151.5	[57]
	commercial activated carbons	250	[58]
	Cynara cardunculus	333	[59]
	White pine sawdust	102	[60]
	Atriplex Halimus	289.8	This study
BB	commercial activated carbons	312	[58]
	agri-food waste (date stones)	9.12	[61]
	Acivated carbon	34.2	[61]
	Activated carbon from olive cores	77.513	[62]
	Atriplex Halimus	29.7	This study
BR	G2W (Grape Winery Waste).	107.53	[63]
	G2WZnM	117.65	[63]
	agri-food waste (date stones)	20.5	[61]
	Acivated carbon	5.017	[64]
	Atriplex Halimus	32.9	This study

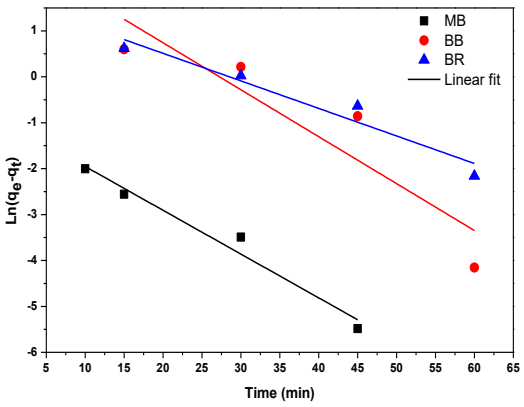

Fig. 9: Model of kinetics according to the pseudo-first-order.

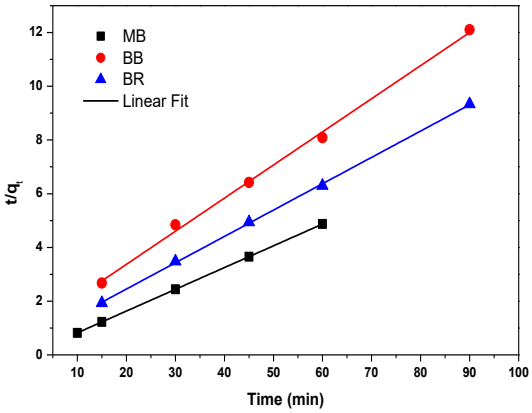

Fig. 10: Model of the kinetics according to the pseudo-second-order.

first-order equation are also largely different from those obtained experimentally, which confirms that the first-order model does not obey this kinetics.

On the contrary, those calculated with the pseudo-second-order equation are quite close to the experimental results. This reveals a limiting step of the adsorption process, and that the adsorption mechanism is characterized by the mass transfer to the surface of the adsorbent [33].

The values of the external diffusion constant k_{id}, as well as those of R^2, are given in Table 5. From this figure, it is easy to see that intra-particle diffusion is a non-negligible step in the adsorption process for all three dyes on the biosorbent. The surface chemical reaction, which begins within the first few minutes of contact and whose experimental points align to pseudo-second-order with very high R^2 regression coefficients, indicates that the most influential step in the adsorption of the dye

Table 5: Kinetic parameters of adsorption of Methylene Blue, Bimacid Blue, and Bimacid Red on the biosorbent (Atriplex Halimus).

	Pseudo-first-order				Pseudo-second-order			Intra-particle diffusion		
dyes	$q_{e(exp)}$ (mg/g)	$q_{e1(cal)}$ (mg/g)	k_1	R^2	$q_{e2(cal)}$ (mg/g)	k_2	R^2	k_i	C	R^2
MB	12.32	0.368	0.0953	0.9589	12.34	0.6075	1.0000	0.0282	12.115	0.8599
BB	7.437	16.21	0.1022	0.7602	8.108	0.0168	0.9968	0.3549	4.3728	0.8553
BR	9.643	5.578	0.0599	0.9128	10.20	0.0197	0.9998	0.3395	6.6776	0.8916

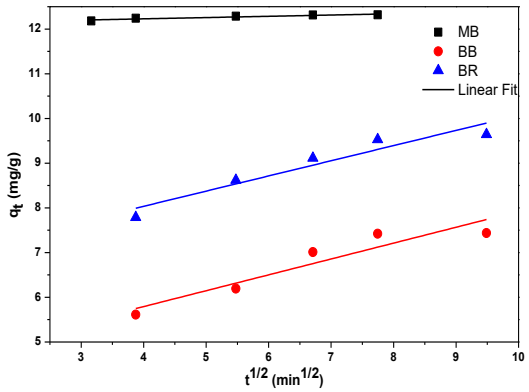

Fig. 11: Model of the kinetics according to the intraparticle diffusion.

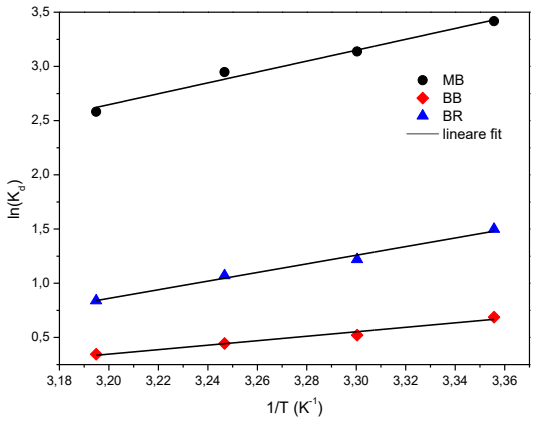

Fig. 12: Evolution of Ln(Kd) as a function of (1/T) for the adsorption of Methylene Blue, Bemacid Blue, and Bemacid Red by Biosorbent.

onto the biosorbent remains the intra-particle diffusion process since it can be considered as a limiting step that controls the rate of dye transfer at each time t. This also confirms that the adsorption of MB, BB and BR is a multi-step process (two differentiated steps are detected) involving adsorption on the external surface and inward diffusion [66].

Study of the influence of temperature

The temperature plays an important role in determining the adsorption process [1]. Fig. 12 and Table 6 build the results obtained for the three dyes (Methylene Blue, Blue Bemacid and Red Bemacid) on the Biosorbent (Atriplex Halimus), and the latter shows us that the increase of the temperature caused an adsorption [67]. The evolution of Ln(K_d) as a function of (1/T) (Fig. 12) allowed us to deduce the thermodynamic quantities relating to the studied adsorbent/adsorbate systems.

Negative values of ΔG° indicate that the process is feasible and spontaneous while negative values of ΔH° indicate an exothermic process for all three dyes. Finally, negative values of (ΔS°) suggest the probability of thermodynamically favorable adsorption [66].

CONCLUSIONS

This study highlighted the effectiveness of biosorbent based on Atriplex Halimus leaves to remove three dyes methylene blue, Bemacid Blue, and Bemacid Red in the aqueous medium. The material was characterized by determining the iodine value which is an important parameter to judge the microporosity, pH_{PCZ}, Boehm's method to identify the functional groups, and determining the mesoporous surface by Langmuir isotherm. The value of iodine index obtained is 425.2 gm/L, thus indicating the microporosity of biosorbent is significant and the index of methylene blue is 119.5 gm/L.

The study of the adsorption kinetics allowed us to determine the time necessary for the establishment of the adsorption equilibrium, located at 60 min for MB and 90 min for BB and BR. The ratio of adsorbent/adsorbate is 8 g/L for all three dyes. The optimal pH for obtaining a better removal rate is 11 for MB, 6.45 for BB, and 5.12 for BR.

Table 6: Thermodynamic parameters of adsorption of the three dyes (MB, BB, and BR) by Biosorbent (100 mg/L).

Dyes	T (K)	K_d	ΔG (kj.mol^{-1})	ΔH (kj.mol^{-1})	ΔS (kj.mol^{-1}.K^{-1})	R^2
MB	298	30.46	-8.46	-41.73	-111.5	0.9745
	303	23.05	-7.90			
	308	19.07	-7.55			
	313	13.22	-6.72			
BB	298	1,99	-1.70	-17.14	-51.97	0,9649
	303	1.69	-1.31			
	308	1.56	-1.14			
	313	1.41	-0.90			
BR	298	4.48	-3.71	-33.08	-98.70	0.9829
	303	3.38	-3.07			
	308	2.92	-2.74			
	313	2.31	-2.18			

The experimental isotherms show an increase of the adsorbed quantity with temperature. The study of the adsorption isotherms shows that the Langmuir model correctly describes the adsorption process with maximum adsorbed quantities of 289.8 gm/L for MB, 29.7 gm/L for BB, and 32.9 gm/L for BR. They are generally of type L for the three dyes and which results in an adsorption in monolayer with the presence of energetically homogeneous adsorption sites.

To determine the rate and mechanism controlling the biosorption phenomenon, three kinetic models were used: pseudo-first-order, pseudo-second-order, and intraparticle diffusion. The results show that adsorption follows the pseudo-second-order model. This model suggests that adsorption depends on the adsorbate-adsorbent couple.

Concerning the thermodynamic parameters, the negative values of the three parameters ΔH°, ΔG°, and ΔS° of the biosorbent/adsorbate system indicate that the reaction is spontaneous and exothermic and that the order of distribution of the dye molecules on the adsorbent is large compared to that in the solution.

From this study, we can conclude that the Biosorbent based on Atriplex Halimus leaves is effective in removing dyes with significant microporosity and mesoporosity.

Acknowledgments

The authors gratefully acknowledge the support of the Direction of Laboratory of Structure, Elaboration, and Application of Molecular Materials (SEA2M) of the University of Mostaganem, Algeria.

Received: Aug. 6, 2021 ; Accepted: Dec. 13, 2021

REFERENCES

[1] Fisli A., Safitri R.D., Nurhasni S.H., Deswita D., Isotherm, Kinetics and Thermodynamics Adsorption Studies of Dye onto Fe_3O_4 Waste Paper Activated Carbon Composites, *J. Teknologi.*, **83(1)**: 45–55 (2021).

[2] Hejazifar M., Azizian S., Adsorption of Cationic and Anionic Dyes onto the Activated Carbon Prepared From Grapevine Rhytidome,*J. Disp. Sci. Techn.*, **33(6)**: 846-853 (2012).

[3] Jibril M., Noraini J., Poh L.S., Mohammed Evuti A., Removal of Colour from Waste Water Using Coconut Shell Activated Carbon (CSAC) and Commercial Activated Carbon (CAC), *J. Teknologi.*, **60(1)**: 15-19 (2013).

[4] Maurya R., Ghosh T., Paliwal C., Shrivastav A., Chokshi K., Pancha I., Ghosh A., Mishra S., Biosorption of Methylene Blue by De-Oiled Algal Biomass: Equilibrium, Kinetics and Artificial Neural Network Modelling, *PLoS. One.*, **9(10)**: e109545 (2014).

[5] Noreen S., Bhatti H.N., Nausheen S., Zahid M., Asim S., Biosorption of Drimarine Blue Hf-Rl Using Raw, Pretreated, and Immobilized Peanut Hulls, *D. W. T.*, **52**: 7339–7353 (2014).

[6] Ouazani F., Iddou A., Aziz A., Biosorption of Bemacid Red Dye by Brewery Waste Using Single and Poly-Parametric Study, *D. W. T.*, **93**: 171–179 (2017).

[7] Boudechiche N., Mokaddem H., Sadaoui Z., Trari M., Biosorption of Cationic Dye From Aqueous Solutions onto Lignocellulosic Biomass (Luffa Cylindrica): Characterization, Equilibrium, Kinetic and Thermodynamic Studies, *Int. J. Ind.Chem.*, **7 (2)**: 167-180 (2016).

[8] Delali H., Merouani D.R., Aguedal H., Belhakem M., Iddou A., Ouddane B., Valorisation of Waste Mussel Shells as Biosorbent for an Azo Dye Elimination, *Key. Eng. Mat.*, **800**: 187-192 (2018).

[9] Montes-Atenas G., Schroeder S.L.M., Sustainable Natural Adsorbents for Heavy Metal Removal from Wastewater: Lead Sorption on Pine Bark (Pinus Radiata d.Don), *Surf. Interf. Analy.*, **47(10)**: 996-1000 (2015).

[10] Sharafzad A., Tamjidi S., Esmaeili H., Calcined Lotus Leaf as a Low-Cost and Highly Efficient Biosorbent for Removal of Methyl Violet Dye from Aqueous Media, *Int. J. Env. Ana. Chem.*, : 1-24 (2020).

[11] Abdallah M.H.A., Hamieh M., Alameh M., Toufaily J., Rammal H., Étude de L'adsorption Du Bleu De Méthylène Sur Un Biomatériau À Base De L'eucalyptus Selon La Taille Des Particules Treatment of Industrial Wastewater Using a Natural and Biodegradable Adsorbent Based on Eucalyptus, *J. Mater. Env. Sci*, **7(11)**: 4036-4048 (2016).

[12] A. Ouldmoumna L.R., Benderdouche N., Bestani B., Duclaux L., Characterization and Application of Three Novel Biosorbents "Eucalyptus Globulus, Cynara Cardunculus, and Prunus Cerasefera" to Dye Removal, *D. W. T.*, **51**: 3527–3538 (2013).

[13] Kifuani K.M., Mayeko A.K.K., Vesituluta P.N., Lopaka B.I.,Bakambo G.E., Mavinga B.M., Lunguya J.M., Adsorption D'un Colorant Basique, Bleu de Méthylène, en Solution Aqueuse, Sur un Bioadsorbant Issu De Déchets Agricoles de Cucumeropsis Mannii Naudin, *Int. J. Biol. Chem. Sci.*, **12(1)**: 558-575 (2018).

[14] Ardizzone S., Gabrielli G., Lazzari P., Adsorption of Methylene Blue at Solid/Liquid and Water/Air Interfaces, *Colloids. Surf. A: Physicochem. Eng. Asp.*, **76**: 149-157 (1993).

[15] Hegyesi N., Vad R.T., Pukánszky B., Determination of the Specific Surface Area of Layered Silicates by Methylene Blue Adsorption: The Role of Structure, pH and Layer Charge, *Appl. Clay. Sci.*, **146**: 50-55 (2017).

[16] Chemrak M.A., Benderdouche N., Bestani B., Benallou M.B., Cagnon B., Removal of Mercury from Natural Gas by a New Activated Adsorbent from Olive Stones, *Can. J. Chem. Eng.*, **96(1)**: 241-249 (2018).

[17] ASTM, "Standard Test Method for Determination of Iodine Number of Activated Carbon. In *Astm Annual Book*", D 4607–94, (1999).

[18] Douara N., "Adsorption de Composés Phénoliques Par Un Déchet Traité Chimiquement". These Doctorat de l'université de Mostaganem, These Doctorat, Université de Mostaganem, (2015).

[19] Okibe F., Gimba C., Ajibola V., Ndukwe I., Preparation and Surface Characteristics of Activated Carbon from Brachystegia Eurycoma and Prosopis Africana Seed Hulls, *Int. J. ChemTech. Res.*, **5(4)**: 1991-2002 (2013).

[20] Jiao Y., Han D., Lu Y., Rong Y., Fang L., Liu Y., Han R., Characterization of Pine-Sawdust Pyrolytic Char Activated by Phosphoric Acid Through Microwave Irradiation and Adsorption Property Toward Cdnb in Batch Mode, *D. W. T.*, **77**: 247-255 (2017).

[21] Ba S., Ennaciri K.,Yaacoubi A., Alagui A., Bacaoui A., Activated Carbon from Olive Wastes as an Adsorbent for Chromium Ions Removal, *Iran. J. Chem. Chem. Eng. (IJCCE)*, **37(6)**: 107-123 (2018).

[22] Boehm H.P., Some Aspects of the Surface Chemistry of Carbon Blacks and other Carbons, *Carbon*, **32(5)**: 759-769 (1994).

[23] Stevie F.A., Donley C.L., Introduction to X-Ray Photoelectron Spectroscopy, *J. Vac. Sci. Tech. A*, **38(6)**: 063204 (2020).

[24] Termoul M., Bestani B., Benderdouche N., Chemrak M.A., S. A., Surface Modification of Olive Stone-Based Activated Carbon for Nickel Ion Removal from Synthetic Wastewater, *Algerian J. Env. Sc. Tech.*, : (2021).

[25] Dehvari M., Ehrampoush M.H., Ghaneian M.T., Jamshidi B., Tabatabaee M., Adsorption Kinetics and Equilibrium Studies of Reactive Red 198 Dye by Cuttlefish Bone Powder, *Iran. J. Chem. Chem. Eng. (IJCCE)*, **36(2)**: 143-151 (2017).

[26] Elhadj M., Nadjib D., Samira A., Djamel N., Mohamed T., Removal of Maxilon Red Dye by Adsorption and Photocatalysis: Optimum Conditions, Equilibrium, and Kinetic Studies, *Iran. J. Chem. Chem. Eng. (IJCCE)*, **40(1)**: 93-110 (2021).

[27] Radouane L.,Samira A.-N.,Nadjib D., Mohammed M.T.E., Gharib R., Mohamed T., Djamel N., Removal of the Cationic Textile Dye by Recycled Newspaper Pulp and Its Cellulose Microfibers Extracted: Characterization, Release, and Adsorption Studies, *Iran. J. Chem. Chem. Eng. (IJCCE)*, **40(1)**: 133-141 (2021).

[28] Langmuir I., The Constitution And Fundamental Properties of Solids and Liquids. Part I. Solids, *J. Amer. Chem. Soc.*, **38(11)**: 2221-2295 (1916).

[29] Herbert F., Über Die Adsorption in Lösungen. *Zeitschrift für Physikalische Chemie*, **57**: 384-470 (1906).

[30] Jawad A.H., Al-Heetim D.T.A., Abd Rashid R., Biochar from Orange (Citrus Sinensis) Peels by Acid Activation for Methylene Blue Adsorption, *Iran. J. Chemistry. Chem. Eng. (IJCCE)*, **38(2)**: 91-105 (2019).

[31] Douara N., Bestani B., Benderdouche N., Duclaux L., Sawdust-Based Activated Carbon Ability in the Removal of Phenol-Based Organics from Aqueous Media, *D. W. T.*, **57(12)**: 5529-5545 (2015).

[32] Lagergren S., Zur Theorie der Sogenannten Adsorption Gelöster Stoffe, Kungliga Svenska Vetenskapsakademiens, *Handlingar*, **24(4)**: 1-39 (1898).

[33] Ho Y.S., McKay G., Pseudo-Second Order Model for Sorption Processes, *Proc. Biochem.*, **34(5)**: 451-465 (1999).

[34] Song Y. ,Liu Y., Chen S., Qin H., Xu H., Carmine Adsorption from Aqueous Solution by Crosslinked Peanut Husk, *Iran. J. Chem. Chem. Eng. (IJCCE)*, **33(4)**: 69-77 (2014).

[35] Kaparapu J., Krishna Prasad M., Equilibrium, Kinetics and Thermodynamic Studies of Cadmium(ii) Biosorption on Nannochloropsis Oculata, *Appl. Water. Sci.*, **8(6)**: 179 (2018).

[36] Dawood S., Sen T.K., Removal of Anionic Dye Congo Red from Aqueous Solution By Raw Pine and Acid-Treated Pine Cone Powder as Adsorbent: Equilibrium, Thermodynamic, Kinetics, Mechanism and Process Design, *Water. Res.*, **46(6)**: 1933-1946 (2012).

[37] Downarowicz D., Aleksandrzak T., Isobutanol vapor Adsorption on Activated Carbons: Equilibrium and Kinetic Studies, *J. Chem. Eng. Data.*, **62(10)**: 3518-3524 (2017).

[38] Xiao X., Liu D., Yan Y., Wu Z., Wu Z., Cravotto G., Preparation of Activated Carbon from Xinjiang Region Coal by Microwave Activation and its Application in Naphthalene, Phenanthrene, and Pyrene Adsorption, *J. Taiw. Instit. Chem. Eng.*, **53**: 160-167 (2015).

[39] Alslaibi T.M., Abustan I., Ahmad M.A., Foul A.A., Kinetics and Equilibrium Adsorption of Iron (ii), Lead (ii), and Copper (ii) onto Activated Carbon Prepared from Olive Stone Waste, *D.W.T.*, **52(40-42)**: 7887-7897 (2014).

[40] Satya A., Harimawan A., Haryani G.S., Johir M.A.H., Vigneswaran S., Ngo H.H., Setiadi T., Batch Study of Cadmium Biosorption by Carbon Dioxide Enriched Aphanothece Sp. Dried Biomass, *Water.*, **12(1)**: 264 (2020).

[41] Ghoneim M.M., El-Desoky H.S., El-Moselhy K.M., Amer A., Abou El-Naga E.H., Mohamedein L.I., Al-Prol A.E., Removal of Cadmium from Aqueous Solution Using Marine Green Algae, Ulva Lactuca, *Egypt. J. Aquat. Res.*, **40(3)**: 235-242 (2014).

[42] Othman N.,Asharuddin S.M., Cucumis Melo Rind As Biosorbent to Remove Fe(II) and Mn(II) from Synthetic Groundwater Solution, *Adv. Mat. Res.*, **795**: 266-271 (2013).

[43] Rahman N.N.N.A., Shahadat M., Won C.A., Omar F.M., Ftir Study and Bioadsorption Kinetics of Bioadsorbent for the Analysis of Metal Pollutants, *RSC. Adv.*, **4(102)**: 58156-58163 (2014).

[44] Viana R.B., da Silva A.B.F., Pimentel A.S., Infrared Spectroscopy of Anionic, Cationic, and Zwitterionic Surfactants, *Adv. Phy. Chem.*, **2012**: 903272 (2012).

[45] Venkata Ratnam Myneni N.R.K., Vangalapati M., Methylene Blue Adsorption by Magnesium Oxide Nanoparticles Immobilized with Chitosan (cs-mgonp): Response Surface Methodology, Isotherm, Kinetics nd Thermodynamic Studies, *Iran. J. Chem. Chem. Eng. (IJCCE)*, **39(6)**: 29-42 (2020).

[46] Vaghetti J.C.P., Lima E.C., Royer B., Cardoso N.F., Martins B.,Calvete T., Pecan Nutshell as Biosorbent to Remove Toxic Metals from Aqueous Solution, *Sep. Sci. Tech.*, **44(3)**: 615-644 (2009).

[47] Bedane A.H., Guo T.x., Eić M., Xiao H., Adsorption of Volatile Organic Compounds on Peanut Shell Activated Carbon, *Cana. J. Chem. Eng.*, **97(1)**: 238-246 (2018).

[48] Altaher H., Khalil T.E., Abubeah R., The Effect of Dye Chemical Structure on Adsorption on Activated Carbon: A Comparative Study, *Coloration. Tech.*, **130(3)**: 205-214 (2014).

[49] Benallou M.B., Douara N., Chemrak M.A., Mekibes Z., Benderdouche N., Bestani B., Elimination of Malachite Green on Granular Activated Carbon Prepared from Olive Stones in Discontinuous and Continuous Modes, *Algerian J. Env. Sc. Tech.*, **7(1)**: 1698-1706 (2021).

[50] Khenifi A., Bouberka Z., Sekrane F., Kameche M., Derriche Z., Adsorption Study of an Industrial Dye by an Organic Clay, *Adsorption.*, **13(2)**: 149-158 (2007).

[51] Bouberka Z., Khenifi A., Ait Mahamed H., Haddou B., Belkaid N., Bettahar N.,derriche Z., Adsorption of Supranol Yellow 4 gl from Aqueous Solution by Surfactant-Treated Aluminum/Chromium-Intercalated Bentonite, *J. Haz. Mat.*, **162(1)**: 378-385 (2009).

[52] Tezcan Un U.,Atf_ F., Low-Cost Adsorbent Prepared from Poplar Sawdust for Removal of Disperse Orange 30 Dye From Aqueous Solutions, *Int. J. Envi. Sci. Tech.*, **16**: 899-908 (2018).

[53] Giles C.H., Smith D., Huitson A., A General Treatment and Classification of the Solute Adsorption Isotherm. I. Theoretical, *J. Coll. Int. Sci.*, **47(3)**: 755-765 (1974).

[54] Sabrina A., Élimination Des Ions Fe (ii) en Solution Aqueuse Par Adsorption Sur La Poudre D'écorces D'eucalyptus, *J. Mater. Process. Env (ASJP)*, **4(1)**: 26-32 (2016).

[55] Zaheer Z., AbuBaker Bawazir W., Al-Bukhari S.M., Basaleh A.S., Adsorption, Equilibrium Isotherm, and Thermodynamic Studies to the Removal of Acid Orange 7, *Mat. Chem. Phy.*, **232**: 109-120 (2019).

[56] Crini G., Peindy H.N., Gimbert F., Robert C., Removal of c.I. Basic Green 4 (malachite green) from Aqueous Solutions by Adsorption Using Cyclodextrin-Based Adsorbent: Kinetic and Equilibrium Studies. *Sep. Pur. Tech.*, **53(1)**: 97-110 (2007).

[57] Dehghan Abkenar S., Ganjali M.R., Hossieni M., Sadeghpour Karimi M., Application of Copper Vanadate Nanoparticles for Removal of Methylene Blue from Aqueous Solution: Kinetics, Equilibrium, And Thermodynamic Studies, *Iran. J. Chem. Chem. Eng. (IJCCE)*, **38(6)**: 83-92 (2019).

[58] Belayachi A., Bestani B., Bendraoua A., Benderdouche N., Duclaux L., The Influence of Surface Functionalization of Activated Carbon on Dyes and Metal Ion Removal from Aqueous Media, *D. W. T.*, **57(37)**: 17557-17569 (2015).

[59] Ouldmoumna A., Reinert L., Benderdouche N., Bestani B., Duclaux L., Characterization and Application of Three Novel Biosorbents "Eucalyptus Globulus, Cynara Cardunculus, and Prunus Cerasefera" to Dye Removal, *D. W. T.*, ***51***: 3527–3538 (2013).

[60] Salazar-Rabago J.J., Leyva-Ramos R., Rivera-Utrilla J., Ocampo-Perez R.,Cerino-Cordova F.J., Biosorption Mechanism of Methylene Blue from Aqueous Solution onto White Pine (Pinus Durangensis) Sawdust: Effect of Operating Conditions, *Sus. Env.Res.*, **27(1)**: 32-40 (2017).

[61] BOUDIA R., "Etude Comparative De L'élimination De Colorants Textiles Par Deux Adsorbants: Naturel Et Activé". (2021).

[62] Ghania Henini, Ykhlef Laidani, Salah Hanini, Aida Fekaouni, Della K.D., Equilibrium, Thermodynamic and Kinetic Modeling for the Adsorption of Textile Dye (Bemacid Blue) onto Activated Carbon Synthesized from Olive Cores, *Chemistry & Chem. Eng. Biotech. Food. Ind.*, **22(3)**: 271-288 (2021).

[63] Chergui Y., Iddou A., Hentit H., Aziz A., Jumas J.C., Biosorption of Textile Dye Red Bemacid Etl Using Activated Charcoal of Grape Marc (Oenological By-Product), *Key. Eng. Mat.*, **800**: 151-156 (2019).

[64] Boudia R., Mimanne G., Benhabib K., Pirault-Roy L., Preparation of Mesoporous Activated Carbon from Date Stones for the Adsorption of Bemacid Red, *Water. Sci. Tech.*, **79(7)**: 1357-1366 (2019).

[65] Mohd Din A.T., Hameed B.H., Ahmad A.L., Batch Adsorption of Phenol onto Physiochemical-Activated Coconut Shell, *J. Haz. Mat.*, **161(2)**: 1522-1529 (2009).

[66] Mekibes Z., Bestani B., Douara N., Benderdouche N., Benzekri-Benallou M., Simultaneous Activation of Ficus Carica L. Leaves for the Removal of Emerging Pollutants from Aqueous Solutions, *D. W. T.*, **222**: 322-335 (2021).

[67] Belaid K.D., Kacha S., Étude Cinétique et Thermodynamique de L'adsorption D'un Colorant Basique Sur La Sciure De Bois, *J. Water. Sci.*, **24 (2)**: 131-144 (2011).